

## **Chapter - 4**

### **Studies on Magnesium Ion Conducting Composite Gel Polymer Electrolytes**

## **Studies on Magnesium Ion Conducting Composite Gel Polymer Electrolytes**

Gel polymer electrolytes, the excellent substitute of liquid electrolytes, are an important class of material due to their properties which make them suitable for applications in solid state like electrochemical devices, e.g. rechargeable batteries, supercapacitors etc. [Song et al 1999; Hashmi 2004; Stephan 2006; Agrawal & Pandey 2008]. The gel polymer electrolytes have several advantages over liquid electrolytes, as discussed in Chapter 1. The risk of leakage is drastically reduced and electrode interfacial contact can be maintained during volumetric changes associated with charge/discharge cycles of the batteries. The ability of the gel electrolytes to act as both separator and electrolyte leads to easy device fabrication with the possibility of miniaturization of devices. However, the main drawback associated with these materials have a tendency to flow, this being deleterious both in terms of conductivity decay and, particularly, of battery reliability and safety. To overcome this problem various approaches are under consideration to assure membranes integrity during operation and storage. The dispersion of ceramic filler particles e.g.  $\text{Al}_2\text{O}_3$ ,  $\text{SiO}_2$ ,  $\text{TiO}_2$ , etc. is one of the most common approaches to improve the mechanical as well as electrochemical and transport properties of the polymer electrolytes [Chung et al 2001; Forsyth et al 2002; Stephan & Nahm 2006]. Such fillers have also been incorporated into gel electrolytes in order to preserve a porous structure that maximizes the adsorption of the liquid electrolyte [Tarascon et al 1996] and to reduce the risk of leakage [Appetecchi et al 2001; Byrne et al 2004; Gentili et al 2007]. The gel electrolytes (filler free and composites) are mostly reported for lithium ion conducting systems. The  $\text{Mg}^{2+}$  ion conducting gel polymer electrolytes are not widely reported except a few systems [Yoshimoto et al 2001; Kumar & Munichandraiah 2000a]. The scientific and technological importance of  $\text{Mg}^{2+}$  ion conducting gel polymer electrolyte has already been described in detail in Chapter 1, Section 1.4.1.

In the present studies, the effect of addition of a micro and nano-sized active filler MgO and nanosized passive filler  $\text{SiO}_2$  in the PVdF-HFP based  $\text{Mg}^{2+}$  ion conducting gel polymer electrolyte has been investigated. The studies have been carried out employing physical techniques namely X-ray diffraction, thermal analysis, infrared spectroscopy, complex impedance analysis, cyclic voltammetry, conductivity and transport number measurements. The details are described in the following sections.

### **4.1 Structural Studies**

#### *4.1.1 X-ray Diffraction (XRD) Studies*

XRD patterns of the solution-cast films of PVdF-HFP, filler-free polymer gel electrolyte [EC:PC (1:1 v/v) + 1.0M  $\text{Mg}(\text{ClO}_4)_2$  + 20 wt.% PVdF-HFP] and composite gel polymer

electrolytes (gel polymer system dispersed with different fillers) are shown in Fig. 4.1. The XRD pattern of pure PVdF-HFP film shows the typical characteristic of a semi-crystalline microstructure, i.e. the co-existence of mixed crystalline and amorphous nature of the material with predominant peaks at  $2\theta = 14.6^\circ$ ,  $17^\circ$ ,  $20^\circ$ ,  $26.6^\circ$  and  $38^\circ$ . The X-ray diffractogram of filler free gel polymer electrolyte shows a broadened peak between  $10^\circ$  and  $30^\circ$ . The PVdF-HFP peak at  $\sim 27^\circ$  is masked in the broad peak and the intense peak at  $\sim 38^\circ$  disappears. These changes reveal clearly that the gel polymer electrolyte is predominantly amorphous and its crystallinity is depressed due to the addition of liquid electrolyte. This indicates that the liquid electrolyte solution most likely blends with the PVdF-HFP at

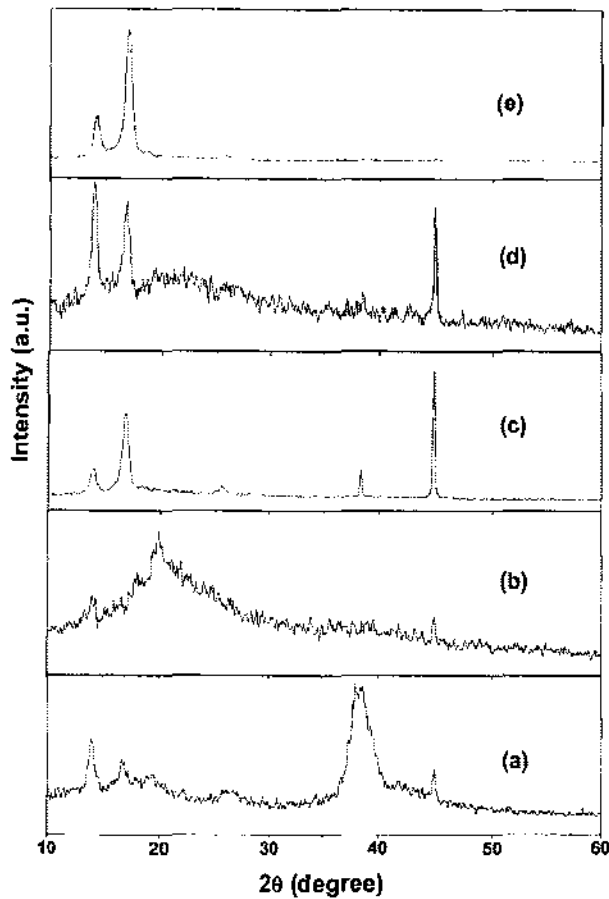


Fig. 4.1: XRD patterns of PVdF-HFP film (a) and gel polymer electrolyte films containing: no filler (b); 10 wt.% micro-sized MgO (c); 10 wt.% nanosized MgO (d) and 10 wt. % nanosized SiO<sub>2</sub> (e).

molecular level and functions as a plasticizer for the polymer. The diffractogram of composite gel polymer electrolyte dispersed with micro and nano-sized MgO shows the characteristic peaks of MgO, observed at  $38.6^\circ$  and  $44.4^\circ$  along with some PVdF-HFP peaks (Fig. 4.1 c and d). In case of nanosized SiO<sub>2</sub> dispersed composite polymer gel electrolyte,

characteristic peak of  $\text{SiO}_2$  has been observed at  $25.5^\circ$  alongwith PVdF-HFP peaks. These observations confirms the composite nature of the all the composite gel electrolyte films.

#### 4.1.2 Scanning Electron Microscopy (SEM) and Atomic Force Microscopy (AFM)

The morphology of the undispersed gel polymer electrolyte and composite gel polymer electrolyte films (with 10 wt.% micro and nano-sized MgO and 10 wt.% nanosized  $\text{SiO}_2$ ) have been examined by SEM and the images are shown in Fig. 4.2. The undispersed gel polymer electrolyte film is observed to have uniform small pores at microscopic level (Fig. 4.2a). The uniform dispersion of micro- and nano-sized MgO particles can be observed and pores are not seen distinctly (Fig. 4.2 b and c). In the case of micro-sized MgO, the particles

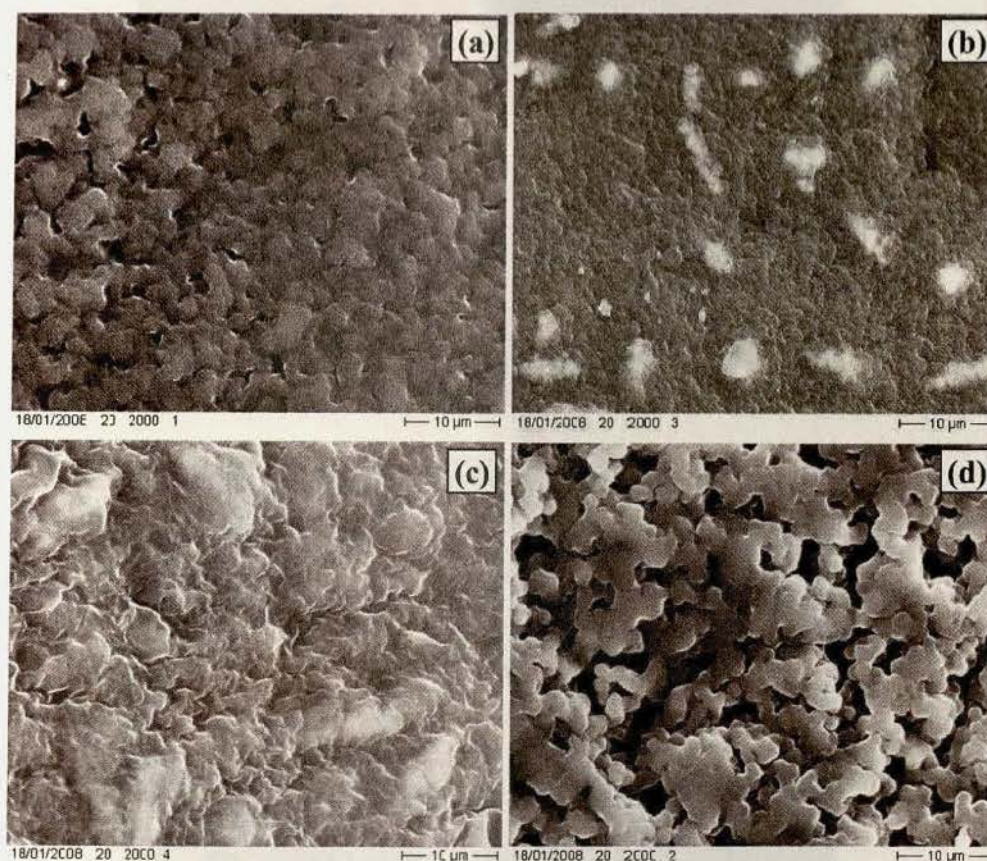


**Fig. 4.2:** SEM images of gel polymer electrolyte films containing (a) 0 wt.% filler; (b) 10 wt.% micro-sized MgO; (c) 10 wt.% nano-sized MgO and (d) 10 wt.% nanosized  $\text{SiO}_2$ .

aggregates are clearly seen. In the composite gel polymer electrolyte dispersed with nanosized  $\text{SiO}_2$ , slightly larger in size and uniformly distributed pores are observed (Fig. 4.2d). The uniformly dispersed pores in the polymer microstructure lead to the retention of

liquid electrolyte and formation of their better connectivity through the polymer, giving rise to high ionic conductivity (discussed below in Section 4.3.1a).

In order to examine the surface morphology at microscopic level further, AFM images of nanosized MgO dispersed nanocomposite gel polymer electrolyte films were recorded and typically shown in Fig. 4.3. The surface has been observed to be almost flat and uniform without pores or any phase separation, which is the indicative of high affinity of polymer host, PVdF-HFP with the liquid electrolyte.

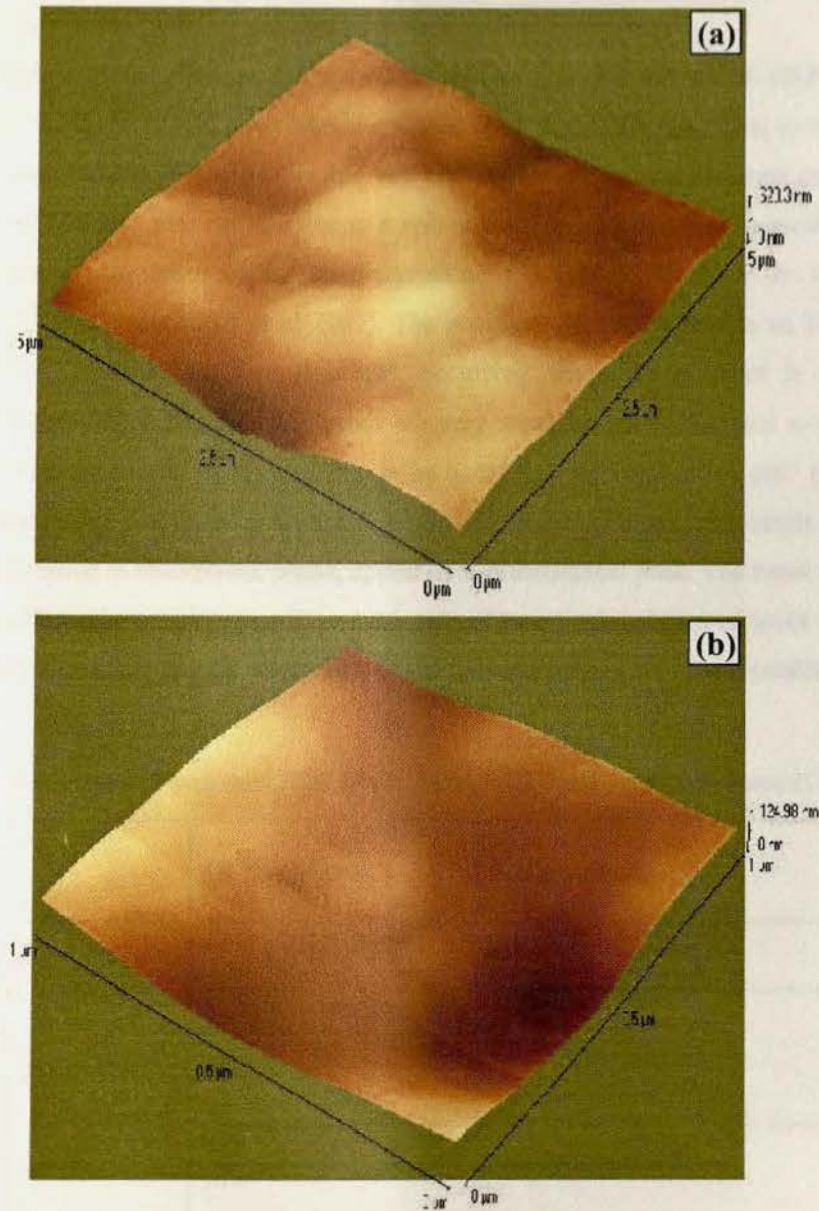


Fig. 4.3: AFM images of the nanocomposite gel polymer electrolyte films containing: (a) 3 wt.% MgO and (b) 10 wt.% MgO.

4.1.3 Fourier Transform Infra-red (FTIR) Spectroscopic Studies

In order to investigate the ion-polymer interaction and possible conformational changes in the host polymer due to the Mg-salt containing liquid electrolyte entrapment and dispersion of various filler particles, FTIR spectroscopic studies have been carried out. Figs. 4.4, 4.5 and 4.6 show the comparative FTIR spectra of the host polymer PVdF-HFP and gel polymer electrolyte films dispersed with different filler contents (from 0 to 20 wt.%), namely, micro-sized MgO, nanosized MgO and nanosized SiO<sub>2</sub>, respectively. Following distinctive features have been extracted from these spectral responses:

(i) The conformational changes in the semi-crystalline host polymer PVdF-HFP due to the addition of liquid electrolyte have been monitored. The peaks corresponding to the bands at 484, 528 (very weak), 762, 839, 879 and 976 cm<sup>-1</sup> are observed and assigned in Table 4.1. The Peaks at 528 and 976 cm<sup>-1</sup> are due to a non-polar *trans-gauche-trans-gauche'* (TGTG') conformation (i.e. α-phase) of the semi-crystalline PVdF-HFP [Gregorio Jr. et al 1994; Abbrent et al 2001; Martinelli et al 2007]. The peak at 484 cm<sup>-1</sup> is due to an intermediate polar TTTG'TTTG' conformation (γ-phase), occurring when the polymer is moderately stressed [Tripathy et al 1979]. Other bands are very weak and/or overlapped with the band associated with the EC-PC or Mg-salt. It may be noted that the band at 762 cm<sup>-1</sup> (assigned to α-phase) disappears due to the addition of liquid electrolyte. Further, the bands at 839 and 879 cm<sup>-1</sup>, assigned to amorphous phase, appear as a symmetrical peak. The band at 879 cm<sup>-1</sup> becomes sufficiently broad, appearing as the sum of two peaks, shown as inset in Fig. 4.4. These observations indicate the substantial conformational changes in the crystalline texture

Table 4.1: Assignment of important FTIR bands of PVdF-HFP and perchlorate anion (ClO<sub>4</sub><sup>-</sup>).

	IR bands (cm <sup>-1</sup> )	Assignment
PVdF-HFP	484	γ-phase
	528 (very weak) 762 976	α-phase
	839 879	amorphous phase
	(ClO <sub>4</sub> ) <sup>-</sup>	ν <sub>4</sub> (ClO <sub>4</sub> ) <sup>-</sup> ion pairs/aggrergates

of the host polymer PVdF-HFP due to the interaction with liquid electrolyte. The disappearance of some bands associated with crystalline  $\alpha$ -phase and appearance of the bands of amorphous phase of the polymer indicate the reduction of crystallinity and dominance of the amorphous phase in the composite gel polymer electrolytes.

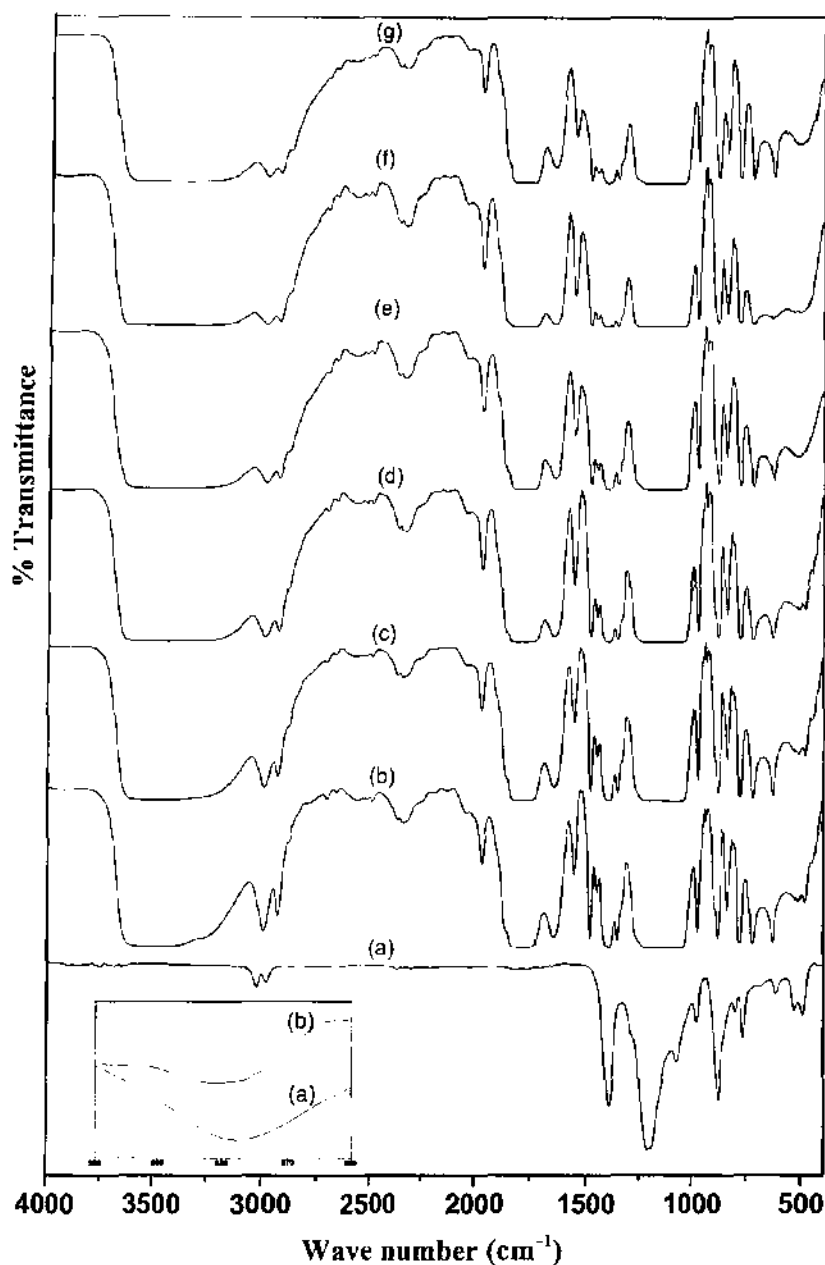
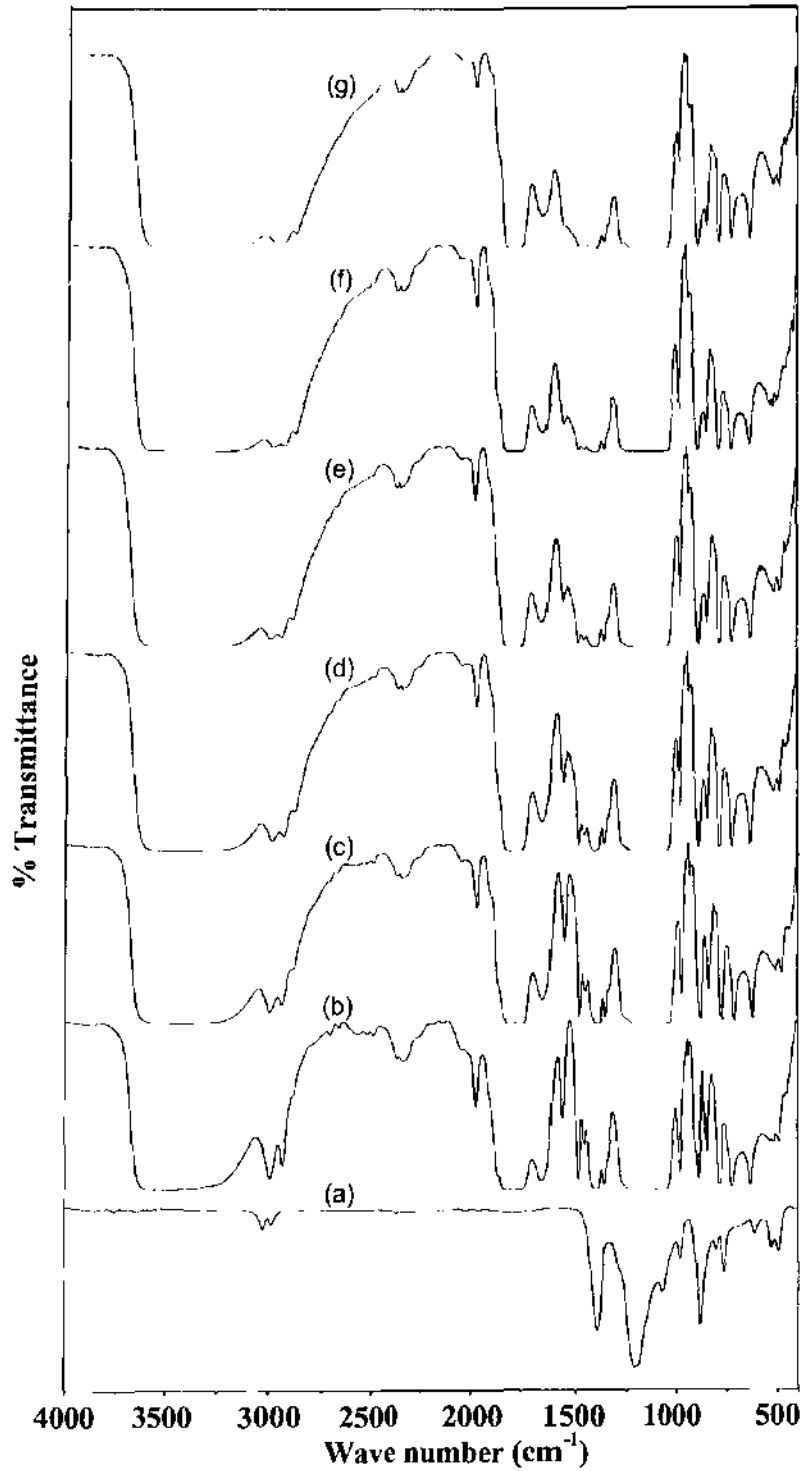


Fig. 4.4: FTIR spectra of (a) PVdF-HFP (pure) film and gel polymer electrolyte films containing micro-sized MgO particles: (b) 0 wt.%, (c) 3 wt.%, (d) 5 wt.%, (e) 10 wt.%, (f) 15 wt.% and (g) 20 wt.%. Expanded representation of the band of 839 cm<sup>-1</sup> is shown in the inset.



**Fig. 4.5:** FTIR spectra of (a) PVdF-HFP (pure) film and gel polymer electrolyte films containing MgO nanoparticles: (b) 0 wt.%, (c) 3 wt.%, (d) 7 wt.%, (e) 10 wt.%, (f) 15 wt.% and (g) 20 wt.%.



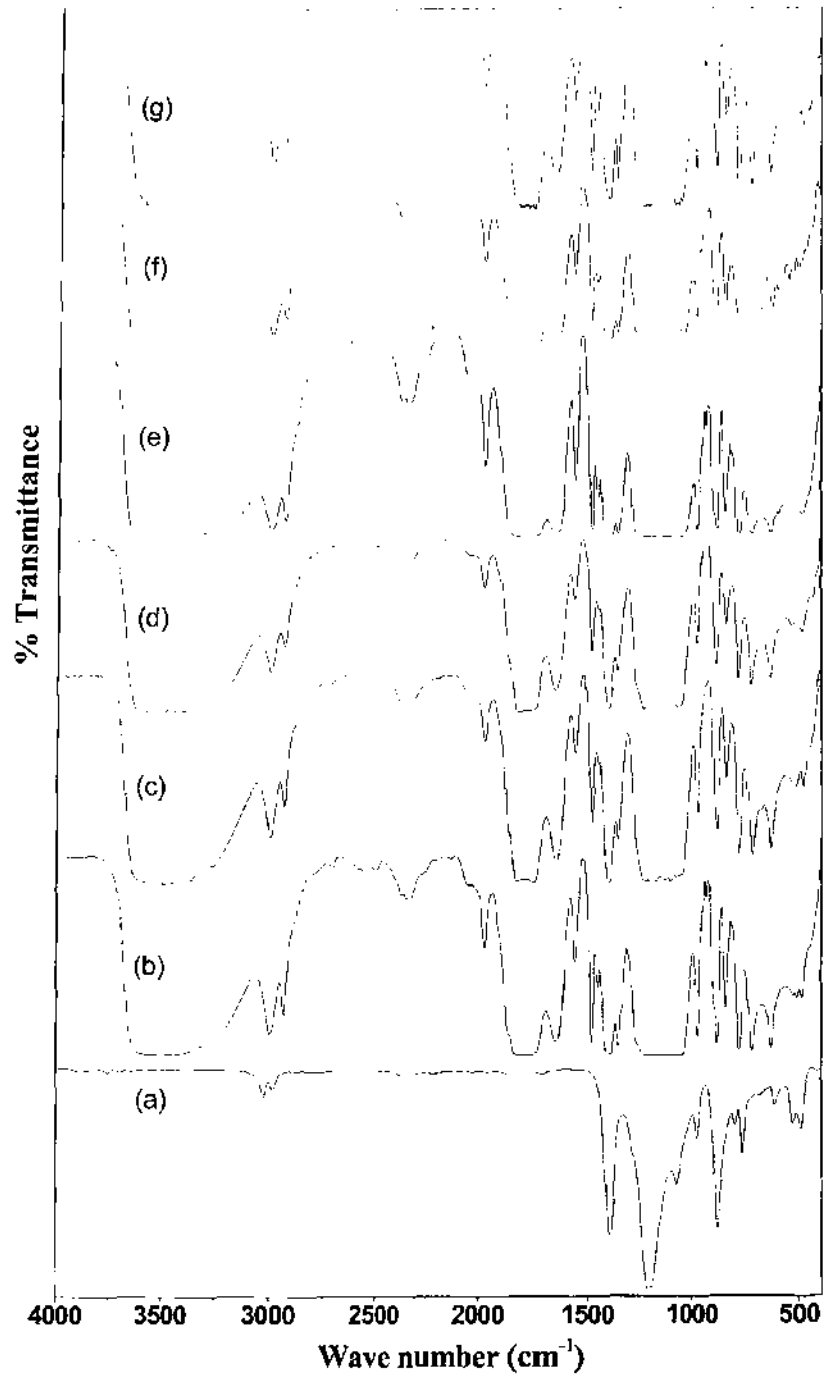


Fig. 4.6: FTIR spectra of (a) PVdF-HFP (pure) film and gel polymer electrolyte films containing SiO<sub>2</sub> nanoparticles: (b) 0 wt.%, (c) 5 wt.%, (d) 7 wt.%, (e) 10 wt.%, (f) 15 wt.% and (g) 20 wt.%.

(ii) The stretching vibration mode ( $\nu_4$ ) of  $\text{ClO}_4^-$  anion observed in the range of  $650\text{-}600\text{ cm}^{-1}$  has been probed to get the information of the degree of salt dissociation in the gel composite polymer electrolyte. The expanded portion of the spectra in the range  $650\text{-}600\text{ cm}^{-1}$  is shown in Fig. 4.7 for different composite gel systems. The peaks at  $\sim 628$  and  $\sim 623\text{ cm}^{-1}$  are attributed to the ion-pair and the free ( $\text{ClO}_4^-$ ) respectively [Chen et al 2002]. In the undispersed gel polymer electrolyte, the peak  $\sim 626\text{ cm}^{-1}$  appeared as the sum of two nearby peaks associated with the free and paired ( $\text{ClO}_4^-$ ) ions. The dispersion of different filler

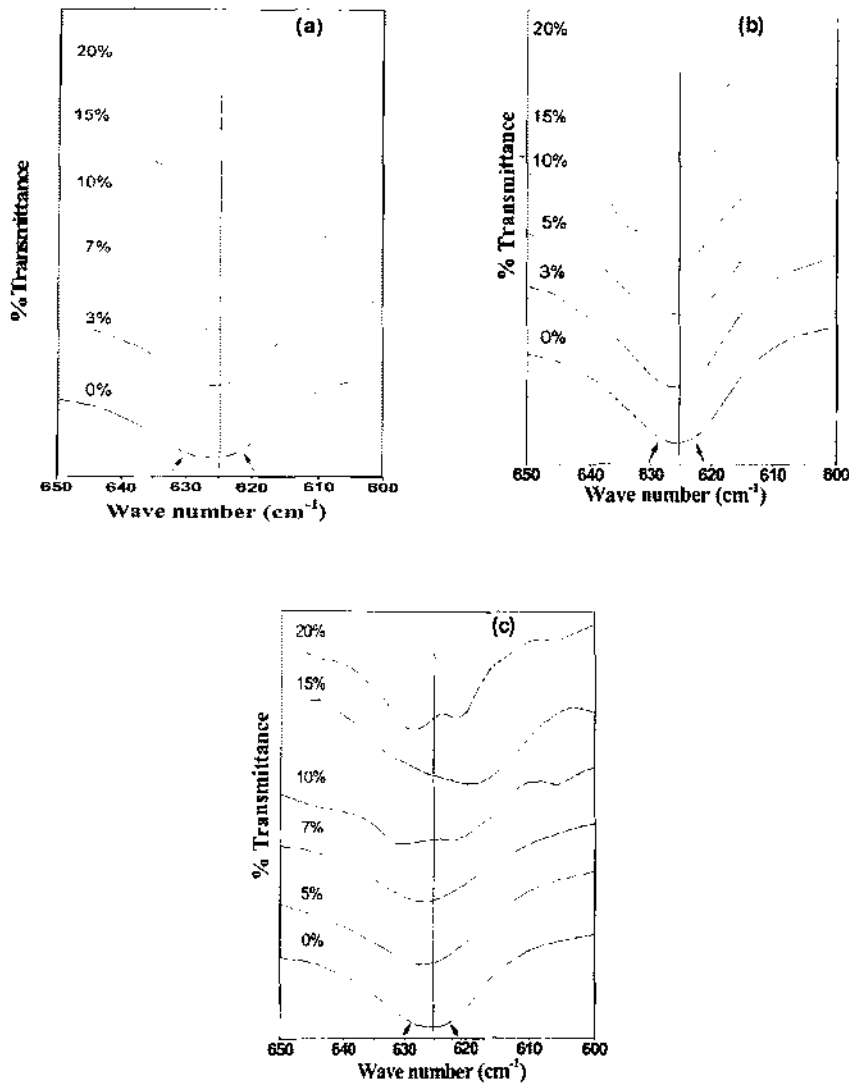


Fig. 4.7: Expanded representation of FTIR spectra of gel composite polymer electrolyte films containing: (a) nanosized MgO, (b) micro-sized MgO and (c) nanosized  $\text{SiO}_2$  filler particles in  $600\text{-}650\text{ cm}^{-1}$  region.

particles in the gel polymer electrolyte influences this band, the peak becomes broader and two peaks appear well separated (Fig.4.7 a-c). This indicates the filler-anion interaction in the composite gel polymer electrolytes.

(iii) It has been observed that the dispersion of MgO nanoparticles in the gel polymer electrolyte also affect the ring stretching and breathing mode of propylene carbonate at  $\sim 932$   $\text{cm}^{-1}$  as obvious from the expanded FTIR spectra shown in Fig. 4.8(a) [Battisti et al 1993]. This band shifts downward with increasing the MgO content. The intensity of broad bands between 2850 and 3050  $\text{cm}^{-1}$  (-CH- stretching mode of the main polymer chain) has been observed to be changed substantially due to the MgO dispersion. The shifts in these bands have also been distinctly observed in Fig. 4.8(b). The dispersion of micro-sized MgO in the gel polymer electrolyte also affect the -CH- stretching mode of the main polymer chain, as shown in Fig. 4.9.

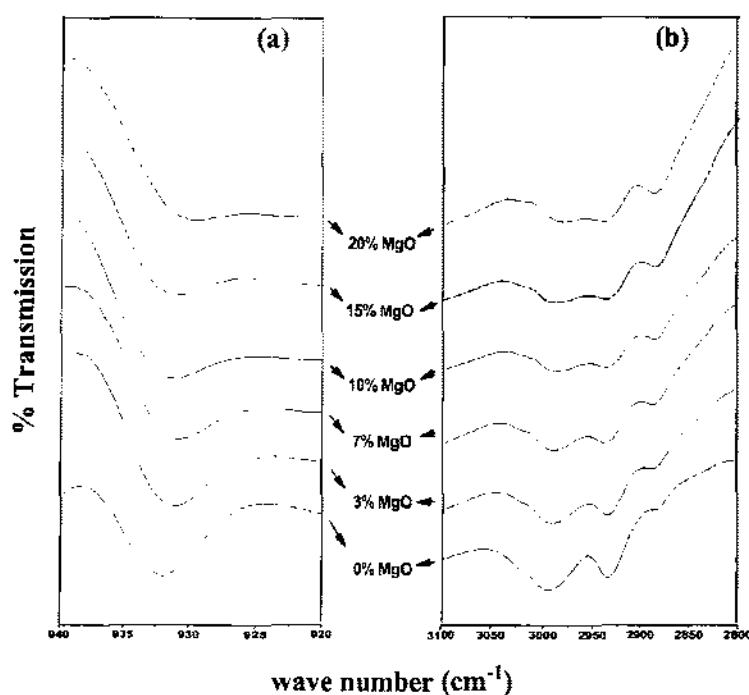
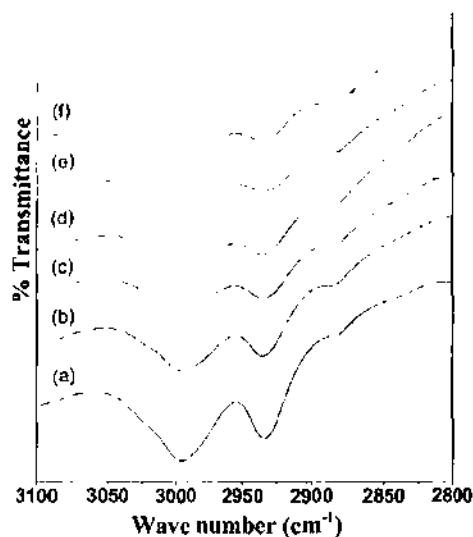
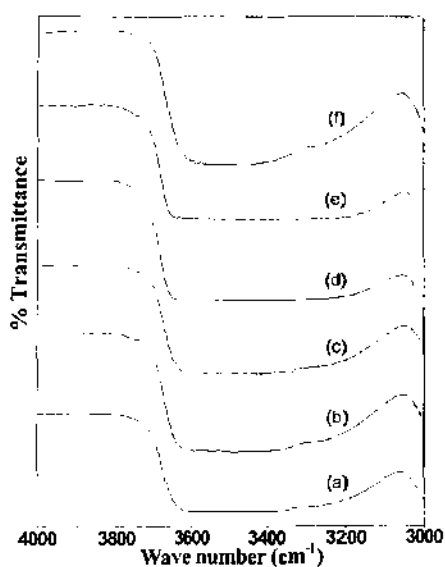


Fig. 4.8: Expanded representation of FTIR spectra of gel polymer electrolyte films containing different amount of MgO nanoparticles in the spectral regions: (a) 920-940  $\text{cm}^{-1}$  and (b) 2800-3100  $\text{cm}^{-1}$ .



**Fig. 4.9:** Expanded representation of FTIR spectra of composite gel polymer electrolyte films containing micro-sized MgO nanoparticles: (a) 0 wt.%, (b) 5 wt.%, (c) 7 wt.%, (d) 10 wt.%, (e) 15 wt.% and (f) 20 wt.% in 2800-3100  $\text{cm}^{-1}$  region.

(iv) The dispersion of  $\text{SiO}_2$  nanoparticles in the gel polymer electrolyte affects the O-H stretching bands. These bands in the region 3660-3230  $\text{cm}^{-1}$  get broadened, creating asymmetric wings toward lower frequency, as shown in the expanded portion (Fig. 4.10).



**Fig. 4.10:** Expanded representation of FTIR spectra of composite gel polymer electrolyte films containing  $\text{SiO}_2$  nanoparticles: (a) 0 wt.%, (b) 5 wt.%, (c) 7 wt.%, (d) 10 wt.%, (e) 15 wt.% and (f) 20 wt.% in 3000-4000  $\text{cm}^{-1}$  region.

This indicates that hydroxyl groups of  $\text{SiO}_2$  are involved in band interactions [Petrowsky & Frech 2003]. It is also likely that the surface hydroxyl groups on different  $\text{SiO}_2$  particles could be hydrogen bonded to one another [Raghavan et al 1998].

These significant changes clearly indicate the substantial modifications in the lattice environment due to dispersion of different filler particles, which in turn affect the ion conduction in the composite gel polymer electrolyte systems significantly.

#### 4.2 Thermal Studies [Differential Scanning Calorimetry (DSC) and Thermo-Gravimetric Analysis (TGA)]

Thermal studies have been carried out on composite gel polymer electrolytes to find out a temperature stability range in which the gel electrolyte can be used safely in the battery like applications. For this purpose, DSC and TGA studies have been carried out. Figs. 4.11, 4.12 and 4.13 show the comparative DSC curves of micro-sized MgO, nanosized MgO and nanosized  $\text{SiO}_2$  containing composite gel polymer electrolytes, respectively. Fig. 4.11a shows the DSC curve of pure PVdF-HFP. The glass transition temperature ( $T_g$ ) has been observed at  $-65^\circ\text{C}$  for pure PVdF-HFP film. After the gel formation due to the addition of liquid electrolyte in host polymer,  $T_g$  value generally decrease, possibly below  $-90^\circ\text{C}$  in the present case, which is not observable due to the limitation of equipment. A step change is

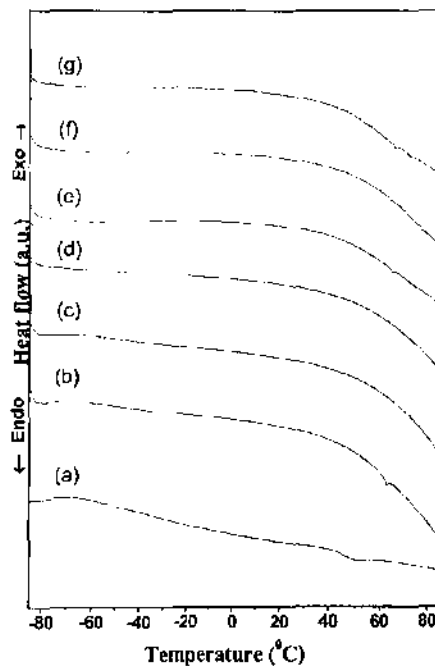


Fig. 4.11: DSC curves of PVdF-HFP (pure) film (a) and composite gel polymer electrolyte films containing micro-sized MgO particles: 0 wt.% (b), 3 wt.% (c), 5 wt.% (d), 10 wt.% (e), 15 wt.% (f) and 20 wt.% (g).

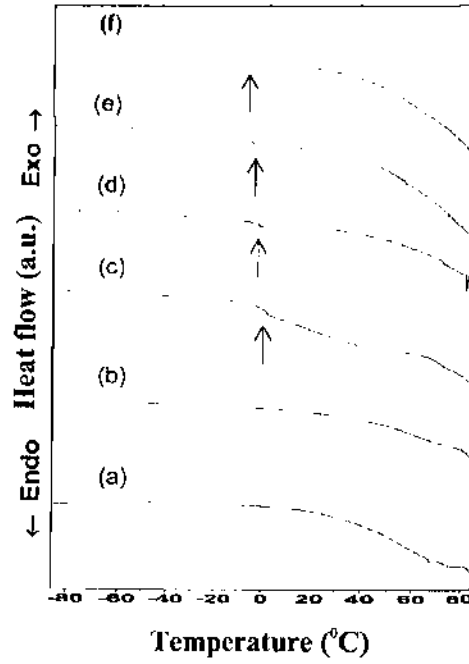


Fig. 4.12: DSC curves of composite gel polymer electrolyte films containing MgO nanoparticles: (a) 0 wt.%, (b) 7 wt.%, (c) 10 wt.%, (d) 12 wt.%, (e) 15 wt.% and (f) 20 wt.%.

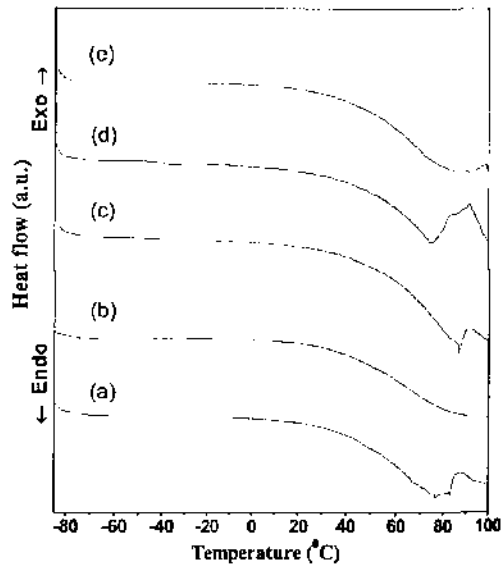


Fig. 4.13: DSC curves of composite gel polymer electrolyte films containing SiO<sub>2</sub> nanoparticles: (a) 0 wt.%, (b) 3 wt.%, (c) 5 wt.%, (d) 10 wt.%, and (e) 20 wt.%.

distinctly observed between 0 and 5°C due to the dispersion of nanosized MgO in nanocomposite gels (Fig.4.12 c-f). This step change is possibly attributed to the glass transition temperature of a separate nanocomposite phase formed due to interaction of MgO nanoparticles with gel polymer electrolyte. Such step changes are not clearly observed for lower contents of MgO nanoparticles (Fig. 4.12 a and b). In case of micro-sized MgO and nanosized SiO<sub>2</sub> dispersion (Fig. 4.11 and 4.13), no such step change has been observed in the composite gel polymer electrolytes. A peak corresponding to melting of the crystalline phase of host polymer PVdF-HFP has been observed ~ 90°C and peak position is almost unaffected due to SiO<sub>2</sub> dispersion (Fig. 4.13). Further, no endothermic peaks have been found and all the three composite gel polymer electrolyte films remains stable in the same gel phase over a wide temperature range from -70 °C to 80 °C, which is a substantial range for their potential applications in electrochemical devices like batteries, etc.

Typical TGA curves of pure PVdF-HFP, undispersed gel polymer electrolyte and composite gel dispersed with micro-sized MgO, nanosized MgO and nanosized SiO<sub>2</sub> filler particles (10 wt.%) are shown in Fig. 4.14. As obvious from Fig. 4.14(a), the host polymer PVdF-HFP exhibit high thermal stability as almost no weight loss has been observed upto ~ 400 °C. A marginal weight loss (~ 5 wt.%) has been observed up to ~ 90 °C for both the

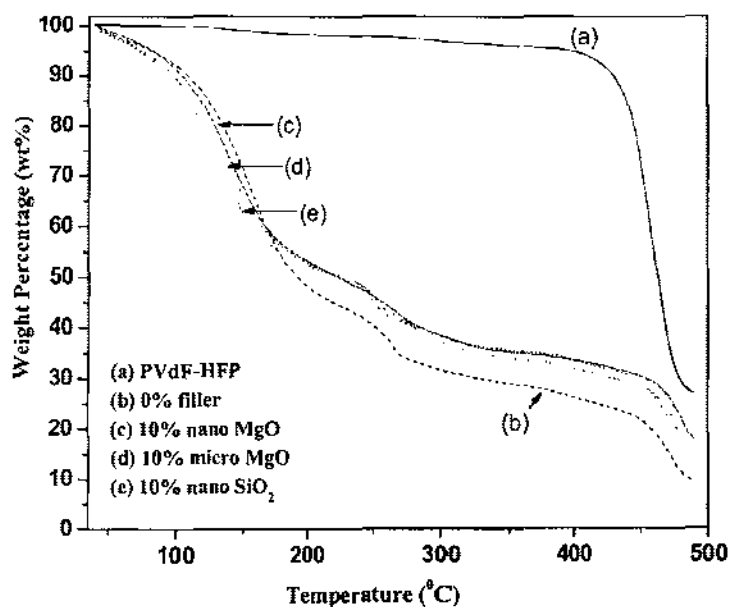


Fig. 4.14: TGA curve of pure PVdF-HFP film and composite gel polymer electrolyte films containing different filler particles.

undispersed and dispersed gel polymer electrolytes, which may be due to the surface adsorbed moisture. Thereafter, a substantial weight loss has started due to the evaporation of the solvents EC and PC. A slightly better retention of EC and PC has been observed, due to the addition of filler particles in composite gel polymer electrolytes.

### 4.3 Electrical Properties

#### 4.3.1 Electrical Conductivity

##### (a) Composition dependence:

Firstly, the composition of gel polymer electrolyte (without fillers) has been electrically optimized. For this purpose, the liquid electrolyte comprising of EC:PC (1:1 v/v) + 1.0 M  $\text{Mg}(\text{ClO}_4)_2$  was added with different amount of PVdF-HFP. Fig.4.15 shows the variation of room temperature ( $\sim 25^\circ\text{C}$ ) electrical conductivity ( $\sigma$ ) as a function of PVdF-HFP content in liquid electrolyte system. The electrical conductivity of liquid electrolyte has been observed to be  $\sim 3 \times 10^{-3} \text{ S cm}^{-1}$ . On addition of host polymer PVdF-HFP, the conductivity initially increases (slightly), shows a maxima ( $\sigma_{\text{max}} \sim 1.06 \times 10^{-2} \text{ S cm}^{-1}$ ) at  $\sim 10$  wt% of polymer and then decreases on further addition of PVdF-HFP. Such conductivity variation phenomenon in the gel polymer electrolytes has been reported earlier by a few research groups [Grillone et al 1999; Chandra et al 2000]. The distinct initial increase in the conductivity due to the addition of host polymer in the liquid electrolyte can be explained by the “breathing polymer

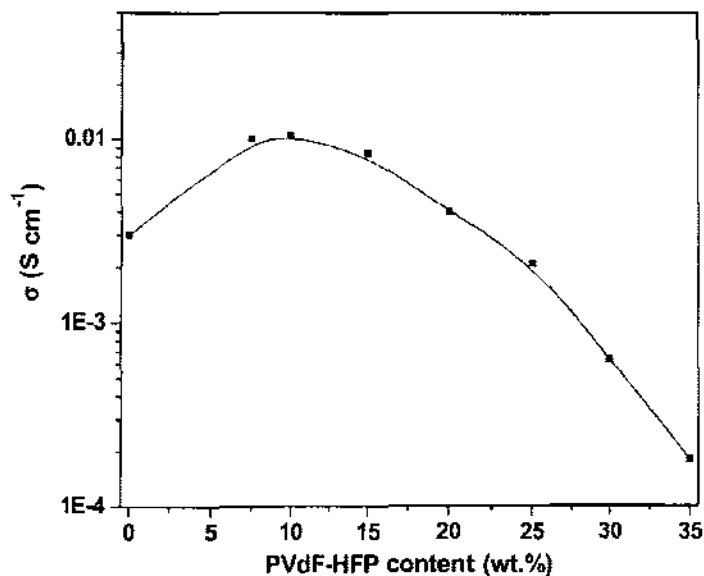


Fig. 4.15: Electrical conductivity of gel polymer electrolytes as a function of PVdF-HFP content.



chain model", suggested by Chandra and coworkers [Chandra et al 2000, 2002]. In this model, the polymer gel is considered to consist of dissociated ions, ion pairs, the solvent and polymer chains (folded or partially/fully unfolded chains). According to this model, the polymer chains are assumed to breathe while they open or fold occupying different volume in the process. This leads to the localized pressure changes or fluctuations assisting either in breaking the ion-pairs or unblocking of the viscosity controlled mobility, both resulting into a conductivity enhancement. It may be interesting to note that the conductivity of the gel electrolyte with 20 wt% of PVdF-HFP has been found to be almost same as that of the liquid electrolyte. Therefore, this composition [EC:PC (1:1 v/v) + 1.0 M  $Mg(ClO_4)_2$  + 20 wt% PVdF-HFP] has been chosen to make composite gel polymer electrolytes, in the form of free standing and mechanically/dimensionally stable films by dispersing different filler particles for their device applications e.g. as separator/electrolyte in Mg-batteries.

The variation of room temperature electrical conductivity of composite gel polymer electrolytes with respect to the content of different filler particles (micro-sized MgO, nanosized MgO and nanosized  $SiO_2$ ) is shown in Fig. 4.16. The addition of different filler particles results an initial increase in the conductivity of gel polymer electrolytes followed by two maxima at ~3 wt.% and ~10-15 wt.% of the filler contents, observed in the conductivity variation in all the three cases. Such two maxima behaviour has recently been reported by

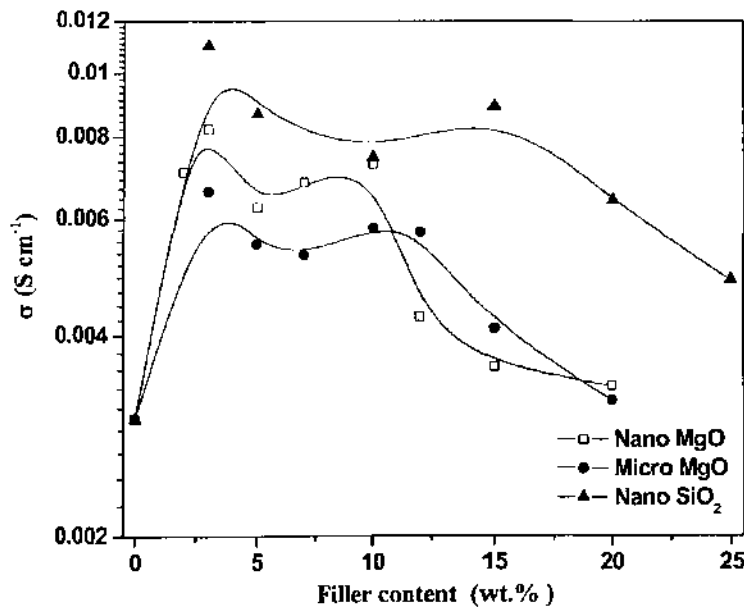


Fig. 4.16: Room temperature conductivity of gel composite polymer electrolyte films as a function of filler content.

few workers for the ion conducting gel polymer electrolyte composites [Sharma & Sekhon 2007] and solvent-free composite polymer electrolytes [Choi & Shin 1996; Hashmi et al 2000; Pandey et al 2008]. The first conductivity maxima is possibly due to the dissociation of ion aggregates/undissociated salt into free ions with the addition of filler particles, whereas the second conductivity maxima is related to the composite effect and explained on the basis of formation of a conducting interfacial space-charge double layer between the filler particles and polymer gel electrolytes [Maier 1994, 1995; Kumar 2004]. The decrease in conductivity after the second conductivity maxima is generally related to the blocking effect of filler particles, which hinders the motion of mobile ions [Kumar et al 2006].

In the case of nanosized SiO<sub>2</sub> dispersion, the conductivity enhancement is little higher as compared to the nanosized MgO dispersion. The maximum conductivity has been found to be  $\sim 1 \times 10^{-2} \text{ S cm}^{-1}$  for 3 wt% of SiO<sub>2</sub> at room temperature ( $\sim 25^\circ\text{C}$ ). This can be explained on the basis of the morphology of two different nanocomposites. As discussed in Section 4.1.2, SiO<sub>2</sub> dispersed nanocomposite gel polymer electrolyte appears to possess more uniformly dispersed pores as compared to nanosized MgO dispersed gel, hence this leads to the high retention of liquid electrolyte and formation of their better connectivity through the polymer, giving rise to high ionic conductivity. Although, the conductivity of nanosized MgO dispersed gel electrolytes is slightly lower, but due to relatively compact morphology observed in this case a substantial improvement in their mechanical strength has been observed. Further, in case of micro-sized MgO dispersed gel electrolyte, the conductivity enhancement is lower than that of nanosized MgO dispersed gel electrolyte, which can be explained in term of the particle size effect of the fillers.

(b) Temperature dependence:

Figs. 4.17, 4.18 and 4.19 show the temperature dependence of electrical conductivity of composite gel polymer electrolyte films dispersed with three different fillers. The ' $\sigma$  vs.  $1/T$ ' plots for gel nanocomposites dispersed with nanosized MgO show linear variation up to  $\sim 60^\circ\text{C}$ , thereafter no conductivity increase has been observed. The linear pattern suggests the Arrhenius-type thermally activated process and can be expressed by following equation:

$$\sigma = \sigma_0 \exp\left(\frac{-E_a}{kT}\right) \quad \text{.....(4.1)}$$

where  $E_a$  is the activation energy,  $\sigma_0$  is the pre-exponential factor and  $k$  is Boltzmann constant. These parameters have been evaluated and listed in the Table 4.2.

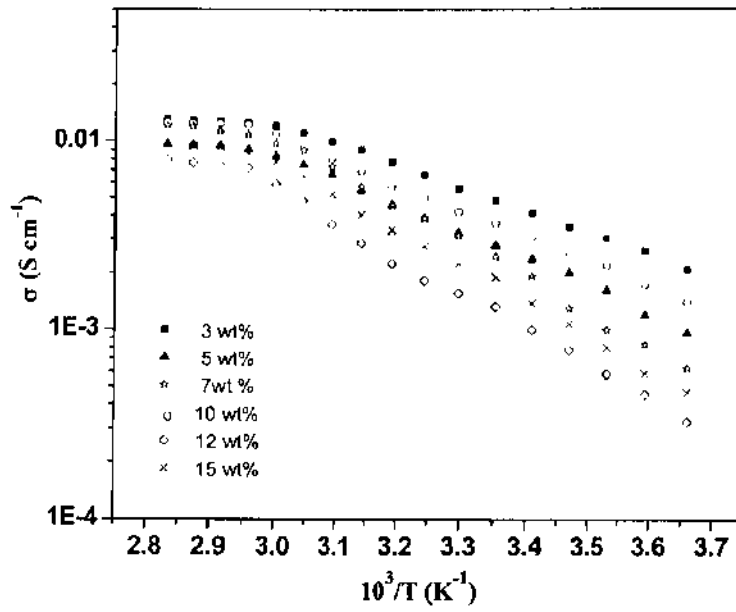


Fig. 4.17: ' $\sigma$  vs.  $1/T$ ' plots of nanosized MgO dispersed composite gel polymer electrolyte films.

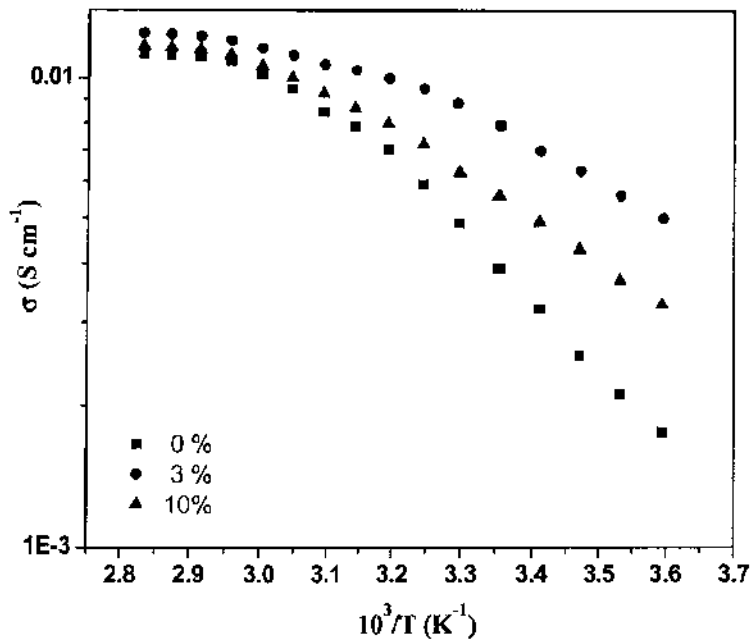


Fig. 4.18: ' $\sigma$  vs.  $1/T$ ' plots of micro-sized MgO dispersed composite gel polymer electrolyte films.

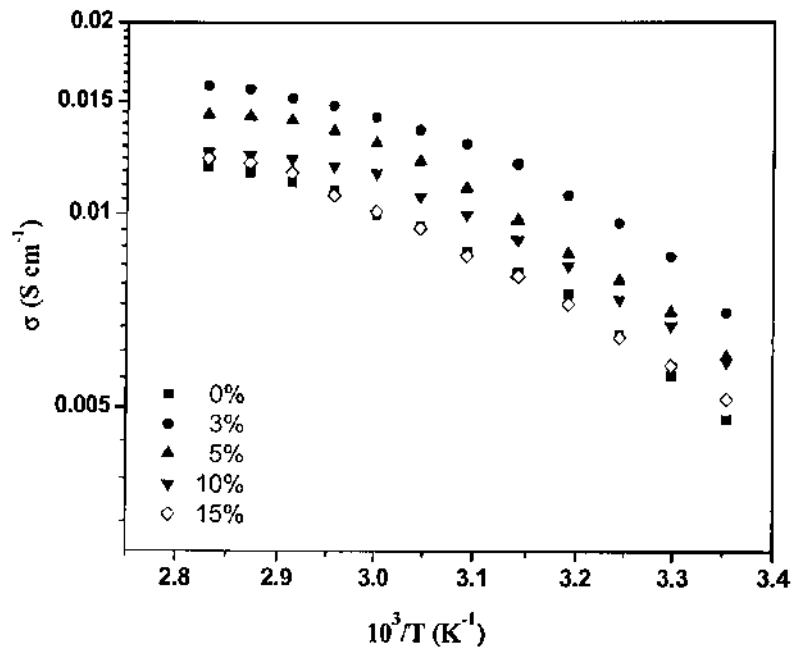


Fig. 4.19: ‘ $\sigma$  vs.  $1/T$ ’ plots of nanosized  $\text{SiO}_2$  dispersed composite gel polymer electrolyte films.

Table 4.2:  $\sigma_0$  and  $E_a$  values for nanosized  $\text{MgO}$  dispersed composite gel polymer electrolyte obtained by linear fitting of conductivity data to Arrhenius equation.

Nanosized $\text{MgO}$ content in gel polymer electrolyte (wt.%)	$\sigma_0$ ( $\text{S cm}^{-1}$ )	$E_a$ (eV)
3	$4.59 \times 10^1$	0.235
5	$4.64 \times 10^1$	0.237
7	$6.82 \times 10^3$	0.383
10	$6.60 \times 10^1$	0.252
12	$2.43 \times 10^3$	0.364
15	$1.02 \times 10^3$	0.350

It has been observed that the ‘ $\sigma$  vs.  $1/T$ ’ curves for the composite gel polymer electrolyte dispersed with micro-sized  $\text{MgO}$  and nanosized  $\text{SiO}_2$  show the non-linear behavior, which follow the Vogel-Tammann-Fulcher (VTF) equation expressed as:

$$\sigma = AT^{-1/2} \exp\left(\frac{-B}{T-T_0}\right) \dots\dots\dots(4.2)$$

where the parameter B has the dimension of energy and is related to the critical free volume for ion transport (although it is not related to any simple activation process), A is a pre-exponential factor i.e. the conductivity at infinitely high temperature and T<sub>0</sub> is equilibrium glass transition temperature close to the T<sub>g</sub> values. These parameters (A, B and T<sub>0</sub>) have been evaluated by non-linear least square fitting of the data and listed in Table 4.3.

**Table 4.3:** A, B and T<sub>0</sub> values for composite gel polymer electrolytes obtained by non-linear least square fitting of conductivity data to VTF equation.

Filler	Filler amount	Parameters		
		A (S cm <sup>-1</sup> K <sup>1/2</sup> )	B (eV)	T <sub>0</sub> (K)
Micro-sized MgO	0	2.51	0.053	179
	3	1.64	0.047	177
	10	1.26	0.032	174
Nanosized SiO <sub>2</sub>	3	1.21	0.022	181
	5	1.33	0.026	178
	10	1.69	0.028	180
	15	2.12	0.032	186

From the temperature dependent electrical conductivity measurements, it can be clearly noted that the optimized Mg<sup>2+</sup> composite gel polymer electrolyte (i.e. with 3 wt% of filler content) exhibits ionic conductivity of the order of ~ 10<sup>-3</sup> S cm<sup>-1</sup> at 0°C and 10<sup>-2</sup> S cm<sup>-1</sup> at 80°C, showing promise for potential application in Mg-batteries in a substantially wider temperature range.

**4.3.2. Transport Number**

The total ionic (cationic + anionic) transport number (t<sub>ion</sub>) has been evaluated using d.c. polarization method, as described in Chapter 2 (Section 2.2.6.2). Fig. 4.20 (a-c) shows 'current vs time' plots for the typical cells: SS | composite gel with 10 wt.% of fillers | SS on applying a voltage of 1.0 V across them. The values of t<sub>ion</sub> have been evaluated using

equation (2.17) and found to be  $> 0.99$  for all the composite gel polymer electrolyte films. This shows that the overall conductivity of the composite gel polymer electrolytes is predominantly ionic and electronic conductivity is negligibly small. No electronic conductivity is expected in the gel-like electrolyte where liquid electrolytes are trapped in the almost inert network of host polymer (PVdF-HFP in the present case) and liquid like charge transport takes place in such systems.

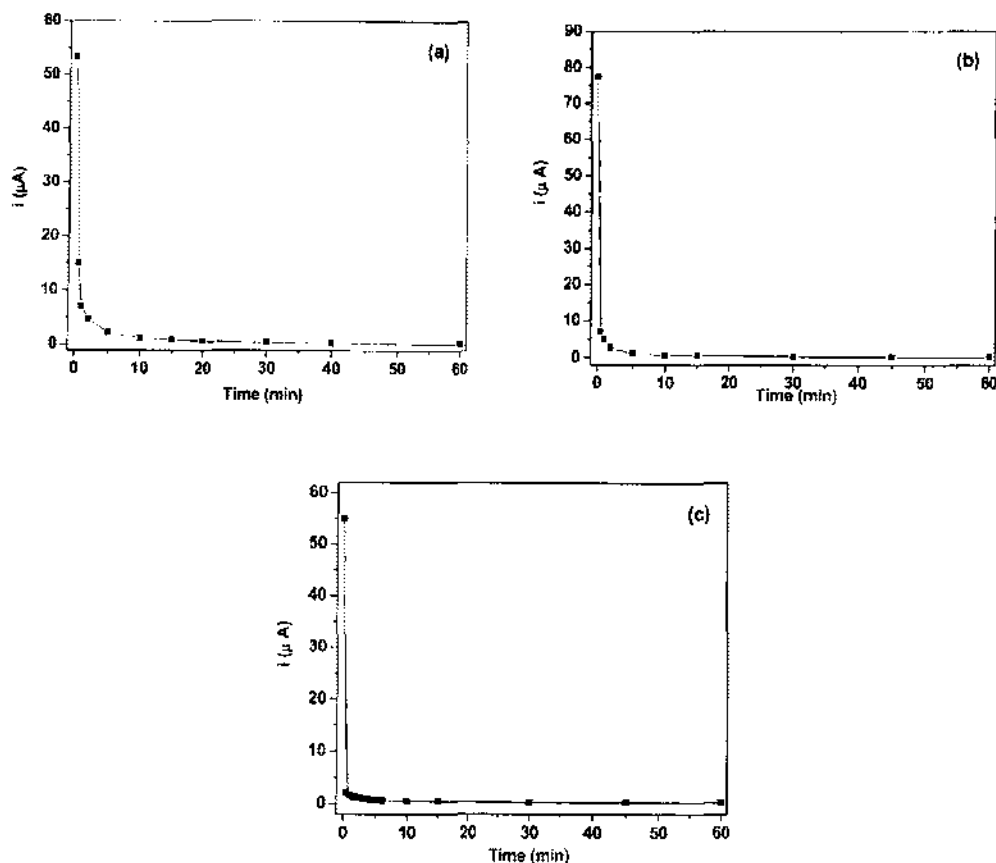


**Fig. 4.20:** ‘Current vs time’ plots for a symmetric cells: (a) SS | composite gel with 10 wt% micro-sized MgO | SS; (b) SS | composite gel with 10 wt.% nanosized MgO | SS and (c) SS | composite gel with 10 wt.% nanosized  $\text{SiO}_2$  | SS at room temperature on applying a potential of 1.0 V.

The cationic transport number at room temperature is a key parameter to evaluate the performance of the electrolytes. In the present case, the transport number ( $t_+$ ) of  $\text{Mg}^{2+}$  ions in the composite gel electrolyte films have been evaluated using the combination of a.c. and d.c. techniques, proposed by Vincent and co-workers [Evans et al 1987], discussed in Chapter 2 (Section 2.2.6.2). In this technique, the cells: Mg | composite gel electrolytes films | Mg were polarized potentiostatically by applying a voltage,  $\Delta V = 0.3$  V for 3-4 hours and

subsequently initial and final currents were recorded. As a part of the technique, the cells were subjected to a.c. impedance measurements prior to and after the polarization. The values of electrode-electrolyte contact resistances were obtained from the impedance plots. The  $t_+$  values were obtained using the equation (2.18).

The typical d.c. polarization curves and a.c. complex impedance plots before and after d.c. polarization of all the cells are shown in Fig. 4.21. The values of  $t_+$  at room temperature, evaluated for all the composite gel polymer electrolyte films for different values of filler contents are listed in Table 4.4.

The value of  $Mg^{2+}$  ion transport number has been found to increase substantially with increasing amount of nano and micro-sized MgO particles up to 10 wt.% (maximum value of  $t_+ = 0.44$  for 10 wt.% nanosized MgO and  $t_+ = 0.39$  for 10 wt.% micro-sized MgO dispersion). Thereafter, the  $t_+$  value has been started slightly decreasing due to the further addition of MgO particles in gel electrolyte system. Further, it may be noted that in case of  $SiO_2$  dispersed composite gel polymer electrolyte, the value of  $Mg^{2+}$  ion transport number does not increase significantly.

The enhancement in cationic transport number with the addition of nanosized inorganic fillers in the PEO based composite polymer electrolytes has been reported by several groups [Capiglia et al 1999; Croce et al 1999; Scrosati 2001]. Scrosati and co-workers [Croce et al 1999; Scrosati 2001] explained the cationic ( $Li^+$  ion) transport number enhancement on the basis of Lewis acid-base reaction between the ceramic surface states and PEO segments, based on the theory proposed by Wicczorek and co-workers [Wicczorek et al 1995; Przyluski et al 1995]. Accordingly, ceramic fillers promote surface conducting pathways due to Lewis acid-base type interaction with PEO segments, through which ions ( $Li^+$  ions) move freely and hence enhancement of the cationic transference number is observed. Further, Kumar and co-workers [Kumar 2004; Kumar et al 2006] has systematically explained the transport mechanism in the colloidal phase of liquid and polymer electrolytes on the basis of space charge double layer formation between ceramic particles and polymer electrolyte surface based on the theory originally proposed by Maier [Maier 1994,1995] for the ionic conduction in solid composites. Accordingly, the space charge regions formed due to the addition of ceramic particles in gel electrolytes are localized sources of electric fields, which influence the movement of charged species. Due to the introduction of ceramic fillers in the gel like electrolytes, the cations may either be transported through the liquid phase of gel polymer electrolyte or through the double layer formed due to the ceramic fillers. The space charge regions (double layers) facilitate the ionic motion and hence, transport number

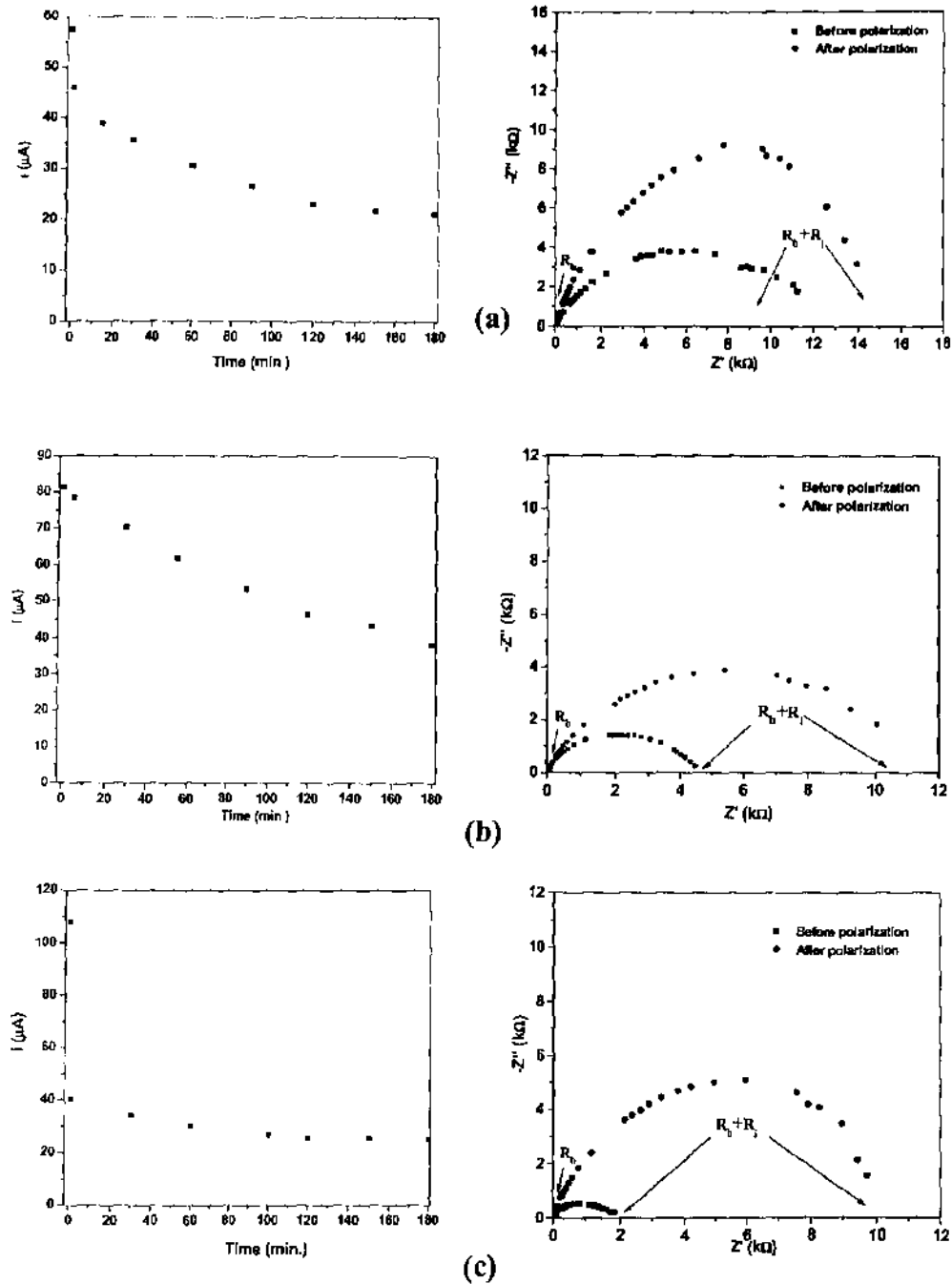


Fig. 4.21: The d.c. polarization ‘current vs time’ plots (left) and the a.c. complex impedance plots before and after d.c. polarization (right) of the cells: (a) Mg | composite gel with 10 wt% micro-sized MgO | Mg; (b) Mg | composite gel with 10 wt% nanosized MgO | Mg and (c) Mg | composite gel with 10 wt% nanosized SiO<sub>2</sub> | Mg at room temperature.



**Table 4.4:** Mg<sup>2+</sup> ion transport number of composite gel polymer electrolytes containing different amount of various filler particles.

Filler	Filler amount (in wt.%)	Mg <sup>2+</sup> ion Transport Number
Micro-sized MgO	0	0.22 ± 0.02
	3	0.28 ± 0.02
	5	0.33 ± 0.02
	10	0.39 ± 0.02
	15	0.30 ± 0.02
Nanosized MgO	3	0.30 ± 0.02
	5	0.36 ± 0.02
	10	0.44 ± 0.02
	15	0.33 ± 0.02
Nanosized SiO <sub>2</sub>	3	0.28 ± 0.02
	5	0.26 ± 0.02
	10	0.28 ± 0.02
	15	0.30 ± 0.02

enhancement is observed. This enhancement effect is observed up to a certain volume fraction of the space charge region. As the volume fraction increases beyond a certain point, space charge regions start giving blocking effect leading to the possible lowering of transport number [Kumar et al 2006].

The materials under the present case, in which nano and micro-sized MgO particles are dispersed in Mg<sup>2+</sup> ion conducting gel polymer electrolytes, are almost similar to the materials studied by Kumar and co-workers [Kumar 2004; Kumar et al 2006]. MgO particles are slightly electronegative in nature and hence, there is a possibility of the following reversible reaction, when these fillers are dispersed in gel electrolyte system:



The  $\text{MgO}:\text{Mg}^{2+}$  species form space charge regions and induce local electric field. This local field is possibly responsible for enhanced  $\text{Mg}^{2+}$  ion motion and hence, enhanced transport number up to the addition of certain extent of filler amount, e.g.  $\sim 10$  wt.% of MgO in the present case. The decrease in the transport number is explained on the basis of the blocking effect of the space charge region due to the further addition of MgO particles [Kumar et al 2006]. As mentioned earlier, no substantial improvement in  $\text{Mg}^{2+}$  ion transport number has been observed due the dispersion of  $\text{SiO}_2$  nanoparticles. This indicates that the space charge region developed due  $\text{SiO}_2$  dispersion, although does not hinder (block) the  $\text{Mg}^{2+}$  ion transport, but it is not much favourable to enhance the cationic transport number. This shows the passive nature of  $\text{SiO}_2$  nanoparticles over the active fillers like MgO for  $\text{Mg}^{2+}$  ion conducting gel polymer electrolytes.

#### 4.4 Electrochemical Studies

##### 4.4.1 Impedance Spectroscopy and Cyclic Voltammetry: Evidence of $\text{Mg}^{2+}$ Ion Conduction

In order to confirm  $\text{Mg}^{2+}$  ion conduction in the composite gel polymer electrolyte films, the complex impedance spectroscopy and cyclic voltammetric studies have been carried out on the symmetrical cells, SS | composite gel polymer electrolytes | SS (Cell-I) and Mg | composite gel polymer electrolytes | Mg (Cell-II). In cell-I, the composite gel films were in contact with the stainless steel (SS, a blocking electrode), whereas foils of Mg were used as reversible electrodes in cell-II. Fig. 4.22 shows the comparative complex impedance plots for Cell-I and Cell-II recorded at room temperature ( $\sim 25^\circ\text{C}$ ) for different composite gel polymer electrolytes. The impedance responses of Cells-I (with SS electrodes) show the steep rising behavior of imaginary impedance at the lower frequency range, indicating the ion blocking nature of the SS electrodes. On the other hand, almost well-defined semicircular dispersion curves have been observed in case of Cells-II (with Mg electrodes). The appearance of the well-defined semi-circle for Mg | composite gel polymer electrolytes | Mg cells clearly suggests that the Mg metal attains equilibrium with the  $\text{Mg}^{2+}$  ions in the composite gel polymer electrolytes. Such behavior has also been reported for Li | gel electrolyte | Li cell [Munichandraiah et al 1997]. The bulk resistance of the gel films ( $R_b$ ) were obtained from the high frequency intercept of the complex plane plots and the interfacial resistance ( $R_i$ ) were calculated from the low frequency intercept. The values of  $R_b$  measured for all the cells have been found to be almost in the same range ( $\sim 15\text{--}40 \Omega \text{ cm}^2$ ) (Fig. 4.22 insets). The value of  $R_i$  for the Mg/composite gel films has been obtained to be  $\sim 3\text{--}12 \text{ k}\Omega \text{ cm}^2$ , whereas for the SS/composite gel films it has been  $\sim 100 \text{ k}\Omega \text{ cm}^2$ . A substantially lower value of  $R_i$

for the Mg/gel composite interface further confirms that equilibrium has been established between Mg metal and  $Mg^{2+}$  ions. These observations confirm  $Mg^{2+}$  ion conduction in the composite gel polymer electrolytes.

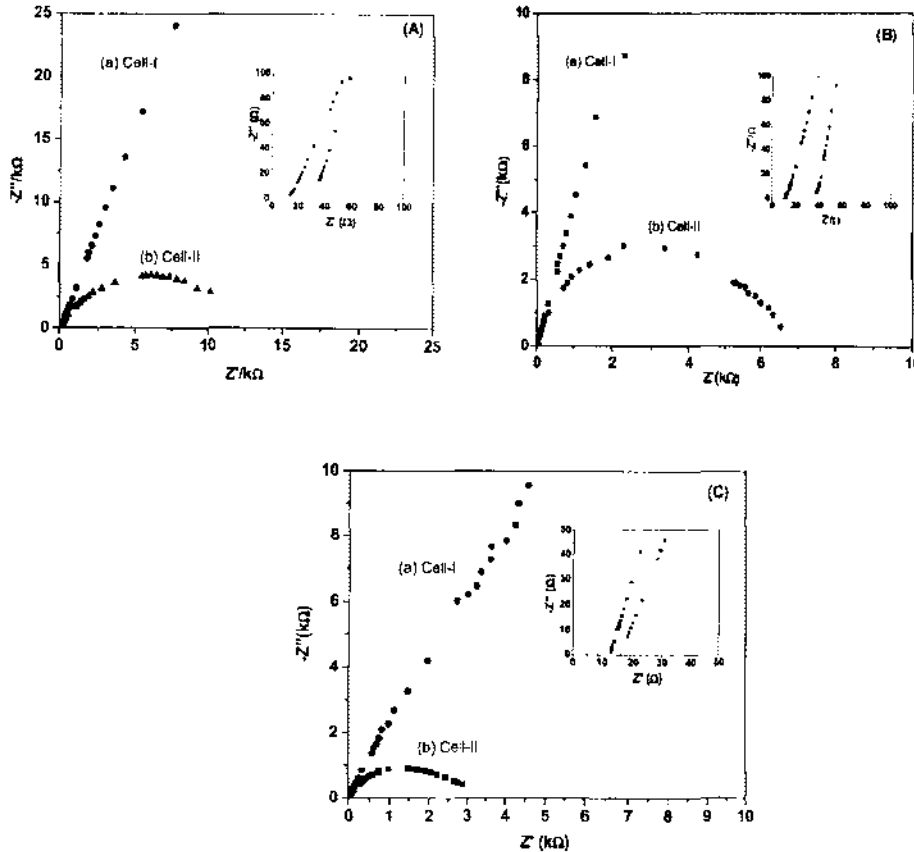


**Fig. 4.22:** Complex impedance plots for: (A) Cell-I: SS|composite gel with 10 wt.% microsized MgO|SS, and cell-II: Mg|composite gel with 10 wt.% microsized MgO|Mg; (B) Cell-I: SS|composite gel with 10 wt.% nanosized MgO|SS, and cell-II: Mg|composite gel with 10 wt.% nanosized MgO|Mg and (C) Cell-I: SS|composite gel with 10 wt.% nanosized SiO<sub>2</sub>|SS, and cell-II: Mg|composite gel with 10 wt.% nanosized SiO<sub>2</sub>|Mg; recorded at room temperature. The high frequency region is expanded and shown as insets in respective figures.

Fig. 4.23 (a-c) shows the cyclic voltammograms (CVs) for the cells containing composite gel electrolyte films with different amount of filler particles sandwiched between two symmetrical Mg-electrodes at a scan rate of  $5 \text{ mV s}^{-1}$ . The CVs of the cells with symmetrical SS electrodes are also shown for comparison. The cathodic and anodic current peaks are distinctly observed for the cells with Mg electrodes, whereas no such features have been observed in case of cells with SS electrodes in the same potential range (Fig.4.23). This suggests the following reversible reaction:

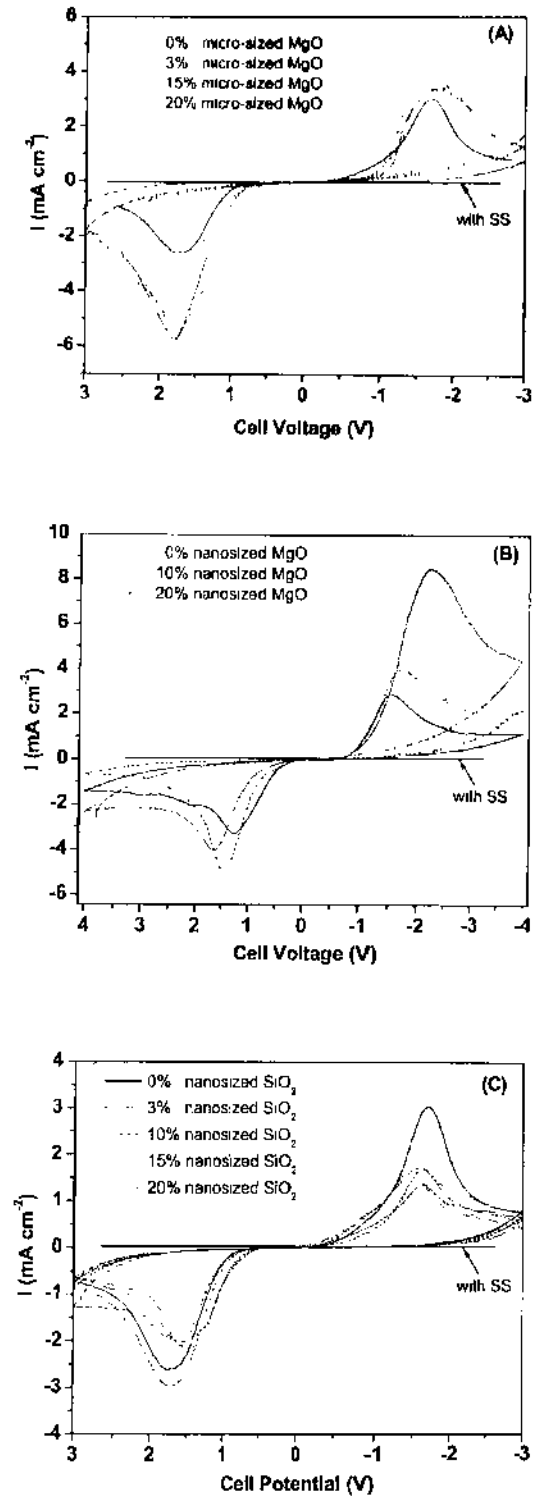


Fig. 4.23: Cyclic voltammograms of cells: (A) Mg| composite gels with micro-sized MgO |Mg; (B) Mg| composite gels with nanosized MgO |Mg and (C) Mg| composite gels with nanosized SiO<sub>2</sub> |Mg recorded at room temperature with scan rate of 5 mV s<sup>-1</sup>.



i.e. the cathodic deposition and anodic oxidation of Mg are facile at Mg/composite gel polymer electrolyte interface. Hence, it is indicative of  $\text{Mg}^{2+}$  ion conduction in the composite gel polymer electrolyte films. It may be noted that the cathodic/anodic peak potentials are separated by several volts, similar to the other cases e.g. Li | PEO+LiBF<sub>4</sub> film | Li cell, reported by Munichandraiah et al. [Munichandraiah et al 2005]. This is possible because the experiments were carried out on the cells with two electrode geometry without using reference electrode. Further, it may be noted that a substantial increase in the anodic/cathodic peak currents has been observed due to the addition of nanosized MgO particles in the gel polymer electrolyte, whereas in case of micro-sized MgO the enhancement in the anodic/ cathodic peak currents is not so pronounced, as typically shown in Fig. 4.24. This result indicates the effective role of smaller (nano) filler particle size for better interfacial

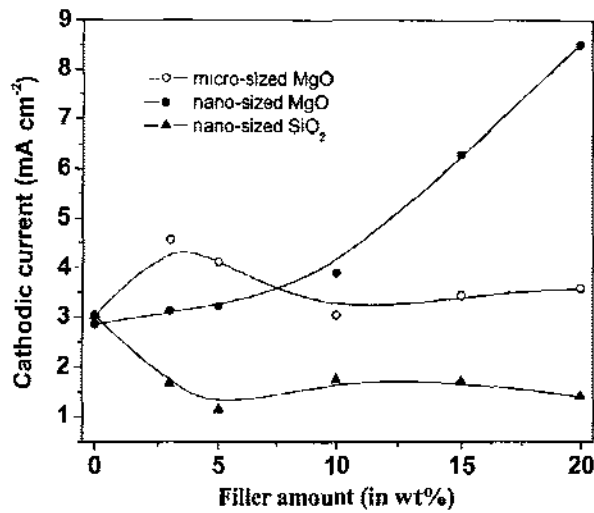


Fig. 4.24: The variation of cathodic current as function of filler content.

activity. On the other hand, an initial decrease in anodic and cathodic currents is observed due to nanosized SiO<sub>2</sub> dispersion upto its ~ 5 wt.% (Fig. 4.24). Thereafter, the current becomes almost constant on further addition of SiO<sub>2</sub>. These variations of current vs. filler content can be explained on the basis of size and nature of space charge regions (double layers), which are formed due to filler dispersion in composite gels following the two considerations:

- (1) MgO particles play the role of active fillers, whereas the SiO<sub>2</sub> particles act as passive fillers dispersed in the composite gel electrolytes.

(2) Size of particles (nano and micro) also play important role in the conduction process of  $Mg^{2+}$  ions.

The interfacial regions (double layers) formed between filler particles and  $Mg^{2+}$  ions are schematically represented in Fig 4.25. The dispersion of nanosized MgO in gel system leads to the formation of larger interfacial area between MgO and  $Mg^{2+}$  ions as compared to the composite gel electrolytes in which micro-sized MgO (~1000 times bigger in particle size) is dispersed. As the MgO particles are active fillers for  $Mg^{2+}$  ion conducting gels, their interfaces with  $Mg^{2+}$  ions support the ionic conduction within interfacial regions. As the interfacial regions are larger in case of nanosized MgO dispersion, the ionic conduction

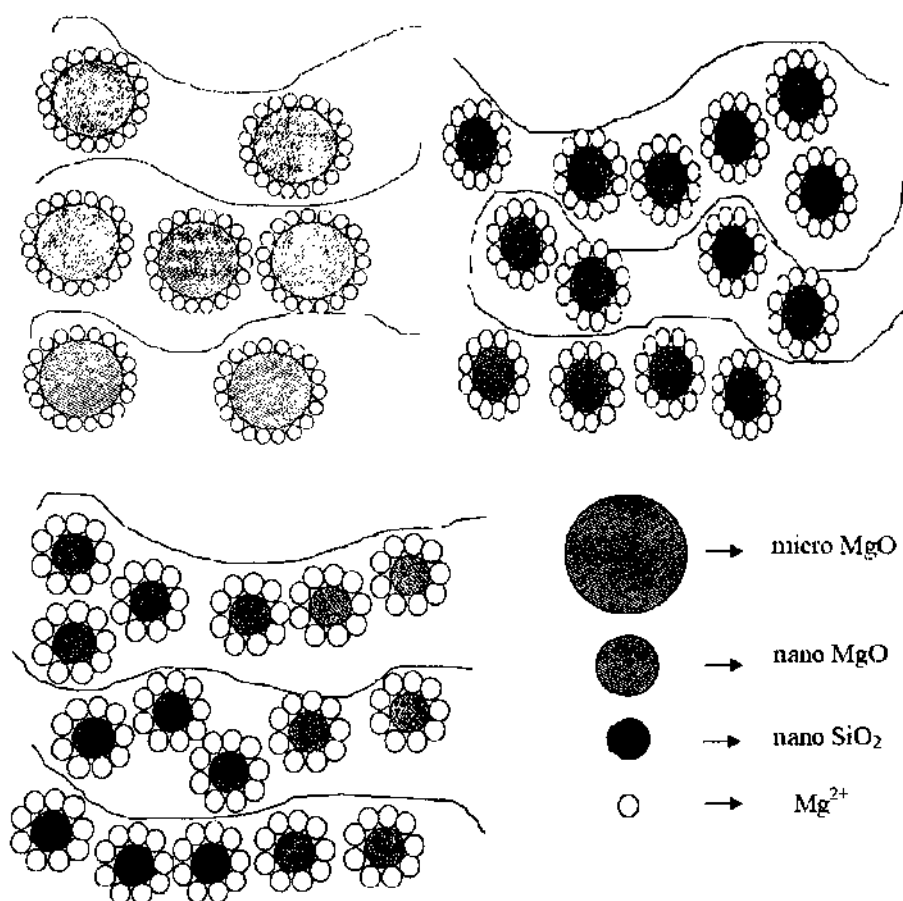


Fig. 4.25: Schematic representation of interfacial regions (double layers) formed between filler particles and  $Mg^{2+}$  ions.

becomes higher and hence cathodic and anodic currents (observed in CV) are larger. Further, in case of dispersion of  $SiO_2$  nanoparticles, although the larger interfacial area is formed between nano  $SiO_2$  and  $Mg^{2+}$  ions, it does not give substantial support to  $Mg^{2+}$  ion conduction. This further indicates the passive role of  $SiO_2$  particles for  $Mg^{2+}$  ion conduction in gel electrolyte.

4.4.2 Electrochemical Potential Window

The electrochemical stability of the composite gel polymer electrolyte films has also been tested using linear sweep voltammetry (LSV) recorded on the cells: SS | composite gel polymer electrolytes | Mg, as discussed in Chapter 2, Section 2.2.6.3. The linear sweep voltammograms for composite gel polymer electrolyte with different filler contents are shown in Fig. 4.26. These LSV records clearly indicate that all the composite gel polymer electrolyte films are stable up to ~3.5 V. The stability has been found to be slightly enhanced

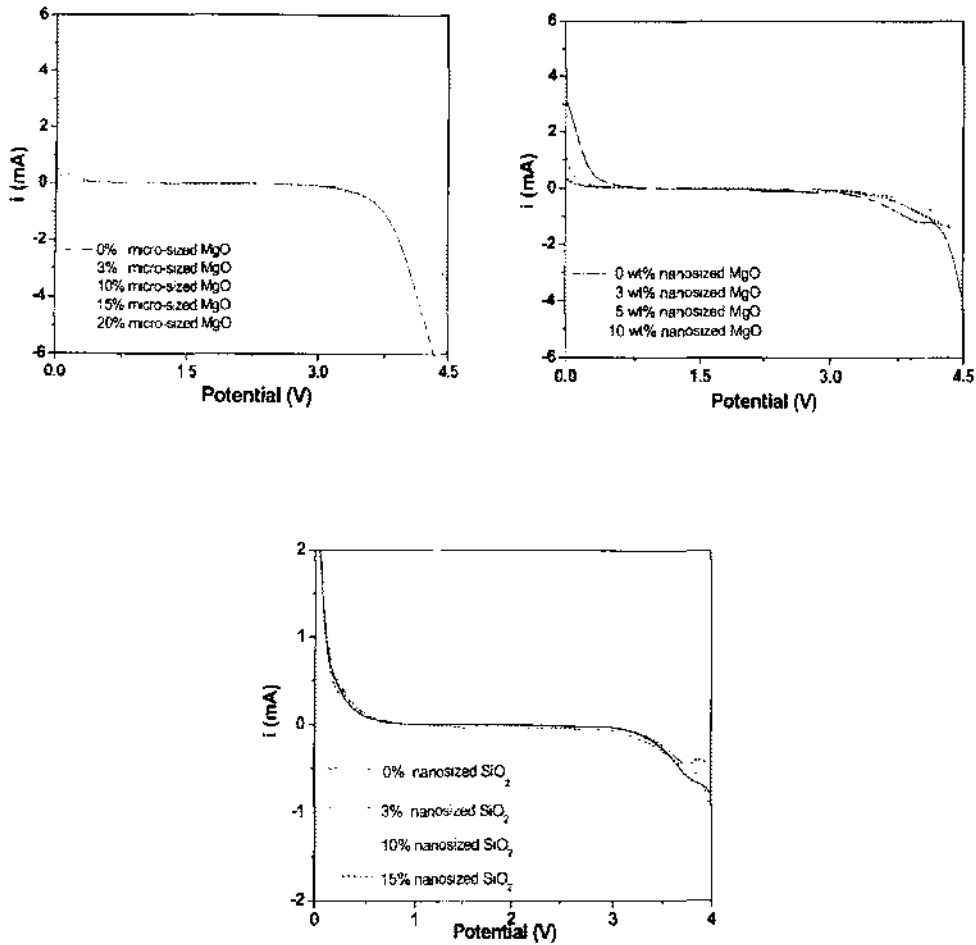


Fig. 4.26: Linear sweep voltammograms of the cells: SS| composite gel polymer electrolyte films |Mg with different filler content recorded at scan rate of  $5 \text{ mV s}^{-1}$ .

due to the addition of filler particles. This value of working voltage range (i.e. electrochemical potential window) is high enough to use the composite gel polymer electrolyte films as solid state like separator/electrolyte in Mg-batteries.

4.4.3 Interfacial Ageing Studies

The electrode/electrolyte interfacial stability is another important aspect to evaluate over a long duration from the battery application point of view. For this purpose, the typical

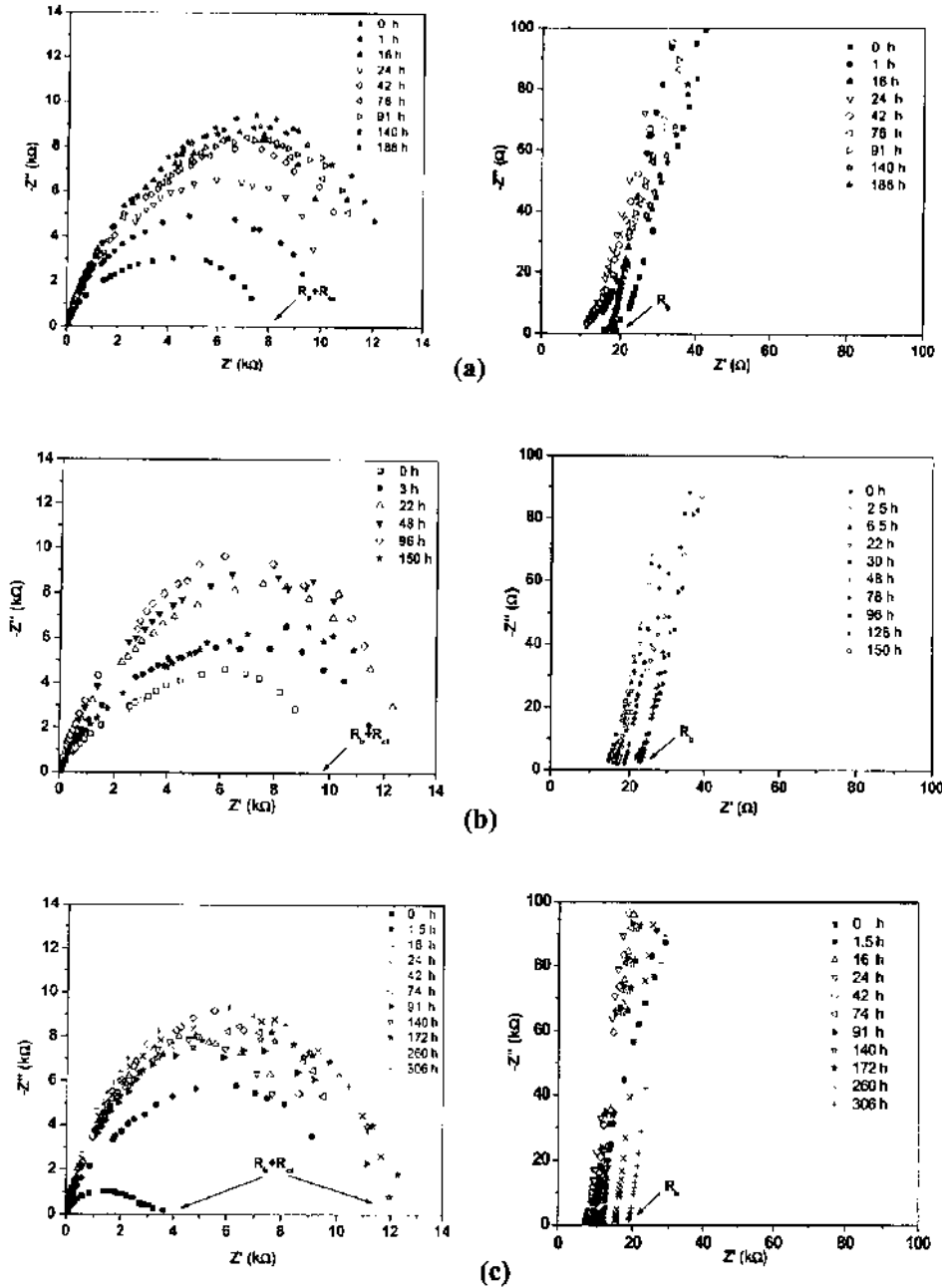


Fig. 4.27: Complex impedance plots of the cells: (a) Mg | composite gel polymer electrolyte with 10 wt.% micro-sized MgO | Mg; (b) Mg | composite gel polymer electrolyte with 10 wt.% nanosized MgO | Mg and (c) Mg | composite gel polymer electrolyte with 10 wt.% nanosized SiO<sub>2</sub> | Mg at different intervals of ageing at room temperature. The high frequency region is expanded and shown on the right side of the figure.



symmetrical cells Mg | composite gel polymer electrolytes | Mg (with the electrolytes dispersed with 10 wt.% of different fillers, micro- and nano-sized MgO and nanosized SiO<sub>2</sub> particles) were assembled and their a.c. impedance spectra were recorded at different time intervals, as shown in Fig. 4.27 (a-c). It has been observed that the size of the semicircles increases with respect to time. Such behavior has also been observed for lithium system (i.e. Li/gel electrolyte interface) [Munichandraiah et al 1997]. An almost stable value of bulk resistance,  $R_b$  (between 12  $\Omega$  to 23  $\Omega$ ) has been observed for more than 100 hours for all the composite gel polymer electrolytes (Fig. 4.27 right figures) and hence, the overall conductivity ( $\sigma$ ) has also been found to be almost constant for quite long time. This indicates that there is insignificant loss of solvent (EC + PC) from the gel electrolytes on ageing. In case of micro-sized MgO dispersed composite gel electrolytes, the charge transfer resistance ( $R_{ct}$ ) increases continuously, whereas in case of nanosized MgO and SiO<sub>2</sub> dispersed composite gel polymer electrolytes the charge transfer resistance ( $R_{ct}$ ) increases initially then becomes constant around 12 k $\Omega$ . This result is attributed to the better interfacial stability due to the incorporation of nanosized filler particles in the gel polymer electrolytes.

#### 4.5 Conclusions

The work reported in this chapter dealt with the characterization of PVdF-HFP based Mg<sup>2+</sup> ion conducting composite gel polymer electrolytes dispersed with micro and nano-sized MgO and nanosized SiO<sub>2</sub> particles. The results confirmed that the addition of nanosized MgO is beneficial in inducing consistent improvements in liquid electrolyte retention as well as in the overall chemical, physical and electrochemical properties as compared to the addition of micro-sized MgO. Various studies like electrical conductivity, transport number measurements, cyclic voltammetry supports that MgO acts as active filler whereas SiO<sub>2</sub> play a role of passive filler in the present composite gel polymer systems. On the basis of various structural, thermal, electrical and electrochemical studies, following conclusions have been drawn:

- (i) The composite nature of the gel polymer electrolyte films due to the dispersion of various filler particles has been confirmed from XRD and SEM studies.
- (ii) Substantial conformational changes in the crystalline texture of the host polymer PVdF-HFP has been observed due to the immobilization of liquid electrolyte in the gel polymer electrolyte. The existence of free anion and filler-polymer interaction has also evidenced from the FTIR studies.

- (iii) The composite gel electrolytes offers high ionic conductivity ( $\sigma \sim 10^{-3} \text{ S cm}^{-1}$  at room temperature) with wider electrochemical potential window and good thermal stability having single phase behaviour for the temperature range from  $-70^{\circ}$  to  $80^{\circ}\text{C}$ .
- (iv) The studies based on the ac impedance spectroscopy and cyclic voltammetry indicated the existence of electrochemical equilibrium between Mg metal and  $\text{Mg}^{2+}$  ions and hence, confirm  $\text{Mg}^{2+}$  ion conduction in the composite gel polymer electrolytes.
- (v) The  $\text{Mg}^{2+}$  ion transport number has become almost doubled due to the addition of 10 wt.% MgO nanoparticles. The enhancement has been explained on the basis of the formation of space charge (double layer) regions due to the presence  $\text{MgO}:\text{Mg}^{2+}$  like species, which supports the  $\text{Mg}^{2+}$  ion motion.

The optimized composite gel polymer electrolyte appears to be an excellent substitute of the liquid electrolyte in electrochemical devices, particularly in the rechargeable magnesium batteries.